ELSEVIER

Ceramics International 31 (2005) 75–80

CERAMICS INTERNATIONAL

www.elsevier.com/locate/ceramint

Effect of Cr_2O_3, Fe_2O_3 and TiO_2 nucleants on the crystallization behaviour of SiO_2–Al_2O_3–CaO–MgO(R_2O) glass-ceramics

M. Rezvani [a,*], B. Eftekhari-Yekta [a], M. Solati-Hashjin [a], V.K. Marghussian [b]

[a] *Material and Energy Research Center, P.O. Box 14155-4777, Tehran, Iran*
[b] *Department of Materials, Ceramics Division, Iran University of Science and Technology, Narmak, Tehran, Iran*

Received 13 January 2003; received in revised form 21 January 2004; accepted 18 March 2004
Available online 28 July 2004

Abstract

The effects of Cr_2O_3, Fe_2O_3 and TiO_2 on the crystallization behaviour of glass compositions in the SiO_2–Al_2O_3–CaO–MgO(R_2O) system were investigated by DTA, XRD and SEM. It was shown that the simultaneous addition of Cr_2O_3, Fe_2O_3 and TiO_2 was more effective in inducing bulk crystallization in these glasses. The Avrami constant, *n*, and activation energy for crystallization of the most promising glass specimens were determined as 3.23 and 253.60 kJ/mol, respectively, suggesting a two-dimensional bulk crystallization mechanism. In this work the best nucleation temperature was determined to be 740 °C. The main crystalline phase detected in the most promising specimens after a two stage 3 h heat treatment at 740 °C and at 885 °C was an aluminium diopside.

Keywords: D. Glass-ceramics; Diopside; Nucleants; Crystallization behaviour

1. Introduction

Developments in the field of production of glass and glass-ceramic articles utilizing inexpensive natural and synthetic materials have been an important advance in glass technology in recent years. The waste materials from metallurgical, mining, chemical and fuel industries and also basalt, oil shales, granite and tuff as inexpensive natural materials served as the starting materials for fabrication of glass ceramics. For example, the slags of iron and steel industry due to the range of their useful physico-chemical and mechanical properties were used in the construction industry as building, facing and lining materials, protective coating against abrasive wear and corrosion in metals, etc. [1–6].

The composition of the above-mentioned glass-ceramics can mainly be located in the SiO_2–Al_2O_3–CaO–MgO system. Many investigators have studied the nucleation process in the SiO_2–Al_2O_3–CaO–MgO and related glass systems. It seems that one of the main difficulties in crystallization of these glasses is initiation of bulk nucleation within them. Cr_2O_3 is one of the most recommended oxides which according to the reports of many researchers is able to induce effective bulk nucleation in the glasses of SiO_2–Al_2O_3–CaO–MgO and related systems. Despite the extensive research work carried out to clarify and explain the role of Cr_2O_3 nucleant in these glasses, still a great controversy existed regarding the exact role of Cr_2O_3 as a nucleating agent, while Williamson [7] found that chromic oxide was not effective as a nucleant in CaO–MgO–Al_2O_3–SiO_2 glass, Shelestak et al. [2,3] introduced Cr_2O_3 as an effective nucleation agent in the CaO–MgO–Al_2O_3–SiO_2 system derived from oil shales and Omar et al. [8] suggested that Cr_2O_3 favours pyroxene crystallization in quartz sand–dolomit–magnesite mixtures. The latter authors also pointed out that iron oxide by enhancing the formation of spinel like nuclei, may assist the crystallization process. Davies et al. [9] suggested that chrome ore is a better nucleant than Cr_2O_3 for the crystallization of glass-ceramics derived from blast furnace slags. They also showed that using pairs of transition metal oxides is more successful than single additions in this connection. Barbieri et al. [10] pointed out that if more than 0.5 mol% Cr_2O_3 is added to glasses of CaO–MgO–SiO_2–Al_2O_3 system, it is precipitated as $MgCr_2O_4$ spinel crystallites in the glass specimens acting as heterogeneous nucleation sites for crystallization of the final diopside and anorthite phases. Their results also

* Corresponding author. Fax: +98-21-8773352.
E-mail address: m_rezvani@scientific.net (M. Rezvani).

0272-8842/$30.00 © 2004 Elsevier Ltd and Techna S.r.l. All rights reserved.
doi:10.1016/j.ceramint.2004.03.037

show that in the case of fine grain glass particles, surface nucleation is predominant even at 5 mol% Cr_2O_3 content, but for coarser particles some degree of bulk nucleation may be observed. Karamanov et al. [11] recognized that Cr_2O_3 is a very effective nucleant in high iron content glasses of SiO_2–Al_2O_3–CaO–Fe_2O_3 system containing small amounts of PbO, ZnO, Na_2O and K_2O. They claimed that 0.7% Cr_2O_3 addition enhances the spinel formation and consequently nucleation rate causing a higher degree of crystallization and finer structures in these glass-ceramics with the major crystalline phase of pyroxene.

Marghussian et al. [12,13] suggested that in the glasses of SiO_2–Al_2O_3–MgO–CaO(R_2O) system, effective nucleation may only occur by using a mixture of Cr_2O_3, Fe_2O_3 and TiO_2.

It seems that the great majority of researchers have rocognized that the presence of transition metal oxides like TiO_2, Fe_2O_3, etc. along with Cr_2O_3 is necessary to render Cr_2O_3 more effective and efficient nucleation agent for crystallization of the above-mentioned glasses. Despite this fact, the exact role of these transition metal oxides in catalyzing bulk nucleation in these glasses still is unclear. Therefore, it was decided to carry out a more comprehensive research work in this connection.

2. Experimental procedure

2.1. Sample preparation

The base glass composition was chosen from a previous work [12,13] as SiO_2 55.05, Al_2O_3 13.61, CaO 24.42, MgO 6.92, Na_2O 2.82 and K_2O 3.02 (weight ratio).

In order to investigate the effect of type and amount of effective nucleants, Cr_2O_3, Fe_2O_3 and TiO_2 were added to the base glass composition in various combinations. Table 1 shows the chemical composition of prepared samples. In Table 1 the base glass composition is labelled as AR.

The raw materials used in the present investigation were reagent grade silica, α-Al_2O_3, $CaCO_3$, $Mg(OH)_2$, Na_2CO_3, Cr_2O_3, Fe_2O_3 and TiO_2.

The mixture of raw materials after thorough mixing were transferred to an alumina crucible and melted at 1450 °C for 2 h in an electric furnace. The melts then were cast into preheated stainless steel moulds and cooled naturally to room temperature. In some cases glass melts were quenched in water in order to prevent the crystallization process.

2.2. Thermal measurements

The thermal behaviour of glasses was monitored by DTA scans which were carried out using a simultaneous thermal analyzer (Polymer Laboratories STA-1640). The heating rate was 10 °C min^{-1} and alumina was used as an inert reference material. Dilatometric softening points (T_d) and crystallization temperatures (T_c) were estimated as well as the shifts of crystallization (exothermic) peaks (ΔT) upon changing the DTA sample particle sizes in The <63 μm and the 0.45–0.55 mm range. Glass transformation temperatures (T_g) and dilatometric softening points (T_d) were also measured by dilatometry (model E-402 Netzsch). Heat treatment of specimens were carried out in a tube electric furnace with a heating rate of 10 °C min^{-1}.

2.3. X-ray diffraction (XRD) and microscopic examinations

In order to determine the crystallization products, the heat-treated samples were subjected to XRD analysis (Siemens, D-500) using Cu Kα radiation at 40 kV and 30 mA setting and in 2θ range from 5° to 65°. The samples after polishing and etching in 5% HF solution for 15–30 s,

Table 1
Chemical composition of prepared glasses (weight ratio)

Oxide	SiO_2	Al_2O_3	CaO	MgO	Na_2O	K_2O	Cr_2O_3	Fe_2O_3	TiO_2
AR	55.05	13.61	24.42	6.92	2.82	3.02	–	–	–
A-Cr_1	55.05	13.61	24.42	6.92	–	–	1	–	–
AR-Cr_1	55.05	13.61	24.42	6.92	2.82	3.02	1	–	–
AR-Cr_3	55.05	13.61	24.42	6.92	2.82	3.02	3	–	–
AR-Cr_5	55.05	13.61	24.42	6.92	2.82	3.02	5	–	–
AR-Fe_1	55.05	13.61	24.42	6.92	2.82	3.02	–	1	–
AR-Fe_3	55.05	13.61	24.42	6.92	2.82	3.02	–	3	–
AR-Fe_5	55.05	13.61	24.42	6.92	2.82	3.02	–	5	–
AR-Ti_1	55.05	13.61	24.42	6.92	2.82	3.02	–	–	1
AR-Ti_3	55.05	13.61	24.42	6.92	2.82	3.02	–	–	3
AR-Ti_5	55.05	13.61	24.42	6.92	2.82	3.02	–	–	5
AR-Cr_3Fe_1	55.05	13.61	24.42	6.92	2.82	3.02	3	1	–
AR-Ce_3Fe_3	55.05	13.61	24.42	6.92	2.82	3.02	3	3	–
AR-Cr_3Fe_5	55.05	13.61	24.42	6.92	2.82	3.02	3	5	–
AR-$Cr_3Fe_5Ti_1$	55.05	13.61	24.42	6.92	2.82	3.02	3	5	1
AR-$Cr_3Fe_5Ti_3$	55.05	13.61	24.42	6.92	2.82	3.02	3	5	3
AR-$Cr_3Fe_5Ti_5$	55.05	13.61	24.42	6.92	2.82	3.02	3	5	5

were coated with a thin film of gold and subjected to microscopic examination by a scanning electron microscope (Cambridge, Stereoscan 360).

3. Results and discussion

Fig. 1 shows the DTA results for most promising specimens exhibiting the sharpest and lowest temperature exothermic peaks among the whole specimens investigated in this work and Table 2 summarizes the DTA results for different particle sizes. It can be seen that the base composition (specimen AR) showing a weak and broad exothermic peak in DTA test is not capable for effective bulk crystallization. The addition of 3 wt.% part Cr_2O_3 to the base composition makes it relatively more susceptible towards bulk crystallization (a relatively sharp peak and low value of ΔT in Fig. 1 and Table 2, respectively).

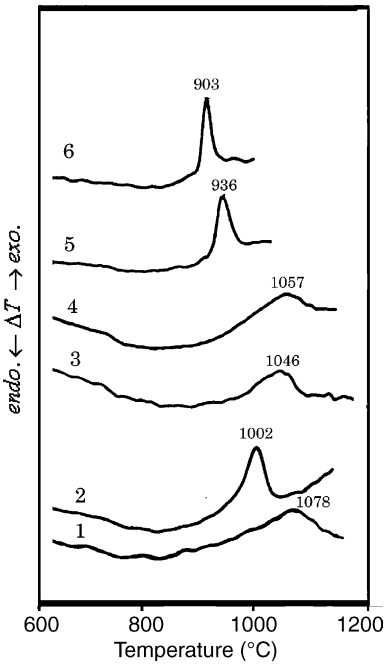

Fig. 1. DTA curves of the most promising glasses AR (1), AR-Cr_3 (2), AR-Fe_5 (3), AR-Ti_5 (4), AR-Cr_3Fe_5 (5) and AR-$Cr_3Fe_5Ti_5$ (6).

Table 2
Summary of DTA results for glass samples of two different particle size distributions

Specimen	Particle size	T_c (°C)	Crystallization peak shift
AR-Cr_3	A	1002	−18
	B	984	
AR-Fe_5	A	1046	−75
	B	971	
AR-Ti_5	A	1059	−71
	B	988	
AR-Cr_3Fe_5	A	936	+4
	B	940	
AR-$Cr_3Fe_5Ti_5$	A	903	+7
	B	910	

A: particle size, 0.45–0.55 mm; B: particle size, <63 μm.

Table 3
Summary of glass transition and crystallization temperatures (T_g and T_c) results for some glass samples

Specimen	T_g (°C)	T_c (°C)
AR	774	1078
AR-Cr_3	805	1002
AR-Cr_3Fe_5	725	936
AR-$Cr_3Fe_5Ti_5$	702	903

The effect of Cr_2O_3 on crystallization of glasses in SiO_2–Al_2O_3–CaO–MgO system have been dealt with many investigators [2,3,10,12–14].

The results can be summarized as follows: Cr_2O_3 after inducing a glass-in-glass phase separation or directly precipitating from molten glass during cooling stage as some form of chromium spinel crystallites, greatly assisted the formation of final pyroxen or diopside-like phases (as heterogeneous nuclei particles).

In the present work in AR-Cr_3 bulk glass specimens some crystalline particles was detected just after cooling in mould. XRD result (Fig. 2) shows the diffraction pattern of the latter specimens exhibiting the faint traces of formation of $MgO{\cdot}Cr_2O_3$ spinel phase. This is consistent with results of other investigators [10,11]. It seems that the tiny spinel crystallites dispersed in the glassy phase also is responsible for considerable rise of T_g in these glasses in comparison to the base glass (Table 3).

The marked nucleating effect of the spinel particles also gave rise to the sharpening of DTA exothermic peak and reduction of T_c by 76 °C (Table 3) and a low ΔT value (Table 2) all indicating the occurrence of a considerable degree of bulk crystallization in these specimens.

The addition of 5 wt.% part Fe_2O_3 and 5 wt.% part TiO_2 to the specimen AR-Cr_3 according to results shown in Table 2 and Fig. 1 resulted in sharper and lower temperature DTA exothermic peaks (an almost 100 °C reduction for coarse particle size specimens in DTA run).

This is a clear indication of the occurrence of more efficient bulk nucleation and crystallization process in the presence of TiO_2 and Fe_2O_3 additives along with Cr_2O_3 nucleant in the glass composition. It also was observed that AR-Cr_3Fe_5 and AR-$Cr_3Fe_5Ti_5$ samples show very low exo-peak shifts in comparison to other specimens (Table 2) verifying the above-mentioned effective bulk crystallization mechanism in these specimens.

Meanwhile the latter samples exhibited positive exo-peak shift values which is unusual. In order to explain this behaviour, AR-Cr_3 and AR-$Cr_3Fe_5Ti_5$ powders (<63 μm particle size) were pressed into disks of 20 mm in diameter and 2 mm in height, heated to the crystallization peak temperatures of 984 and 910 °C, respectively, and then were immediately taken out of furnace. In this way the firing shrinkage

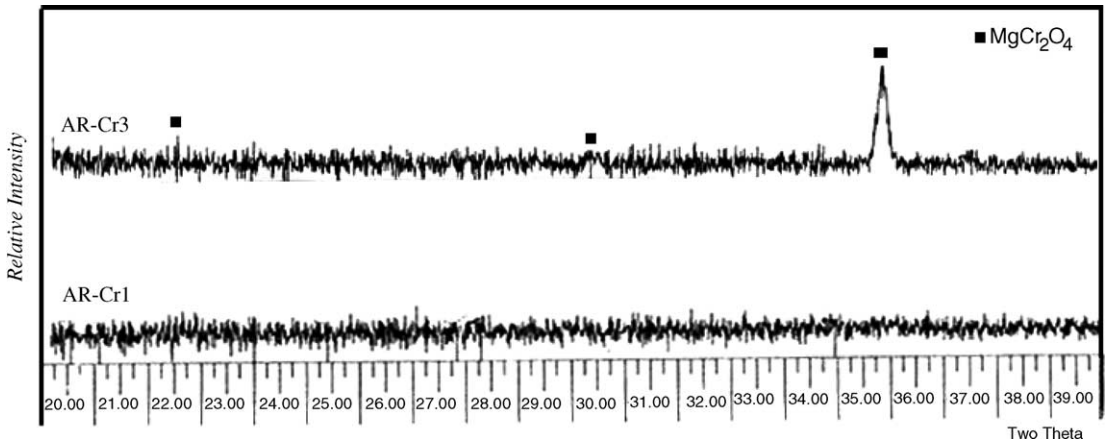

Fig. 2. XRD patterns of AR-Cr_1 and AR-Cr_3 glasses.

of specimens were measured as 6 and 13%, respectively. It can be suggested that the addition of TiO_2 and Fe_2O_3 to the glasses containing Cr_2O_3 has probably reduced the viscosity and increased their sinterability. Therefore, it seems that with increasing the temperature in DTA run the powders, because of their high sinterability, became coarser very rapidly and acted in a similar way to coarse grain samples. Therefore, in the case of powders with high sintering tendencies the comparison of DTA peak shifts for fine and coarse grain samples for prediction of the surface or bulk crystallization mechanism some times may be misleading. The comparison of glass transition temperatures (T_g) (Table 3) again confirms the process of viscosity reduction due to the addition of Fe_2O_3 and TiO_2 additives. It can be seen that the simultaneous addition of 5 wt.% part TiO_2 and Fe_2O_3 causes a nearly 103 °C reduction in T_g. This partly is due to the role of TiO_2 and Fe_2O_3 which probably as network modifiers assuming a co-ordination number of six cations in these glasses in the range of glass transform temperatures [15]. According to Morimoto and Kuriyama [16] because ionic radius of Ti^{4+} is larger than Si^{4+} it prefers octahedral or cubic co-ordination at lower temperatures near the annealing point (at $T < T_g$) of SiO_2–Al_2O_3–MgO–CaO–Na_2O glasses. They concluded that Ti^{4+} ion, which was four-fold co-ordinated at higher temperatures (at $T > T_g$) in some glasses containing relatively lower amounts of R_2O+RO oxides gradually becomes six-fold co-ordinated as nucleation occurred. Therefore, TiO_2 in amounts of >5 wt.% resulted in phase separation or crystallization in such glasses. On the other hand in glasses with relatively large amounts of alkali and or alkaline earth oxides owing to the existence of a large number of non-bridging oxygen ions, Ti^{4+} cations can attain a co-ordination number of 6 and co-ordination change does not occur in them during heat treatment [16].

In this case there is no phase separation and crystallization occurring in glass specimens. It is interesting to note that in the presence of TiO_2 and Fe_2O_3, the 3 wt.% part Cr_2O_3 containing glass specimens as melted and cast in the usual way in metal moulds exhibited no sign of glass-in-glass phase separation or crystallization even in a magnification of 100,000 by TEM. Therefore, it seems that TiO_2 and Fe_2O_3 by providing Cr^{3+} cation-sufficient oxygens to satisfy their co-ordination prevent their separation in any form in the glass specimens.

In our opinion the prevention of Cr_2O_3 to precipitate in the glass matrix as form of chromium spinel crystallites during cooling stage of glass is mainly responsible for reduction of viscosity and lowering of T_g values. In the later stage during the nucleation heat treatment process the high over-saturation of glass specimens in respect to Cr_2O_3 and their lower viscosity accelerates the bulk nucleation and subsequent crystallization processes. Moreover we suggest that the entrance of Fe^{3+} and perhaps Ti^{3+} cations in the structure of $MgO{\cdot}Cr_2O_3$ spinel crystallites, by increasing the unit cell dimensions, reduces the crystallographic mismatch between spinel phase and the final aluminium diopside phase in *a* and especially *b* directions facilitating their nucleation. Table 4 represents the unit-cell dimensions of various spinels (JCPDS 10-351, 21-1152, 21-540) and diopside [12] phases.

In order to confirm the mechanism of crystallization the Matusita method also was used. Matusita and co-workers [17,18] have proposed a method for measurement of activation energy and determination of crystallization mechanism (Avrami constant). They used Eq. (1) that follows:

$$\ln[-\ln(1-x)] = -n\ln\alpha - \frac{1.052mE}{RT} + \text{constant} \qquad (1)$$

Table 4
Unit-cell dimensions of diopside phase and various spinels

Specimen	*a* (Å)	*b* (Å)	*c* (Å)
Ca(Mg, Al) (Si, Al)$_2O_6$ (aluminium diopside)	9.7120	8.8670	5.2660
$MgAl_2O_4$	8.0831	–	–
$FeCr_2O_4$	8.3401	–	–
$MgCr_2O_4$	8.3330	–	–
Mg(Al, Fe)$_2O_4$	8.1905	–	–

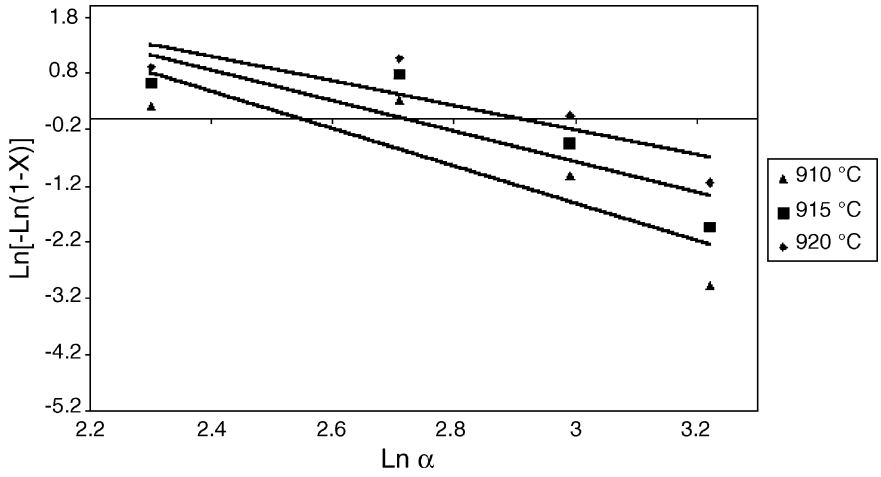

Fig. 3. Variation of $\ln[-\ln(1-x)]$ vs. heating rate logarithm ($\ln\alpha$) in AR-$Cr_3Fe_5Ti_5$.

where x is the fraction transformed (crystal volume fraction) at each temperature that can be measured by the ratio of the partial area to the total area of the crystallization exotherm peak. n = Avrami constant; α = heating rate; T = temperature; R = gas constant and m is a constant that represents the dimensionality of crystal growth. Figs. 3 and 4 show the results of variation of $\ln[-\ln(1-x)]$ versus $\ln\alpha$ and $1/T$ for specimen AR-$Cr_3Fe_5Ti_5$. In this way n and E values were determined as 3.23 and 253.60 kJ/mol, respectively. The Avrami constant, n, indicates a two-dimensional bulk crystallization [14]. Fig. 5 shows SEM micrograph of AR-$Cr_3Fe_5Ti_5$ specimen taken after a two-stage heat treatment. The specimen first was nucleated at 740 °C for 3 h and then heat-treated at 885 °C for 3 h. In order to determine the suitable nucleation temperature first dilatometric analysis was performed on the glass sample. In this way glass transition temperature (T_g) and dilatometric softening point (T_d) were obtained as 702 and 732 °C, respectively. The nucleation process is usually carried out in a temperature range between T_g and T_d. The most suitable nucleation temperature was determined by the Ray and Day method [19]. The most promising glass (AR-$Cr_3Fe_5Ti_5$) samples first were heated at several temperatures such as 700, 720, 740, 750, 760, 780 and 800 °C for 3 h (some of which are located out of the T_g–T_d range) then the DTA test was performed on them. Fig. 6 shows the DTA curves some of samples. According to the results, with increasing the nucleation temperature from 700 to 780 °C in spite of the observed reduction in crystallization temperatures, the sharpness of exo-peaks reduced gradually and eventually at 800 °C the peak was vanished. Therefore, according to this method the most suitable nucleation temperature is 740 °C corresponding to the sharpest DTA exo-peak (at 885 °C). It may be suggested that soaking the specimen at 740 °C only resulted in nucleation and no effective crystallization occurred but the heat treatment at 800 °C brought about considerable crystallization (due to the possible overlap of nucleation and growth versus temperature curves at this temperature) and in the subsequent heating in DTA test due to the previous crystallization and lack of glassy phase no exo-peak was observed. Fig. 7 exhibits the XRD results.

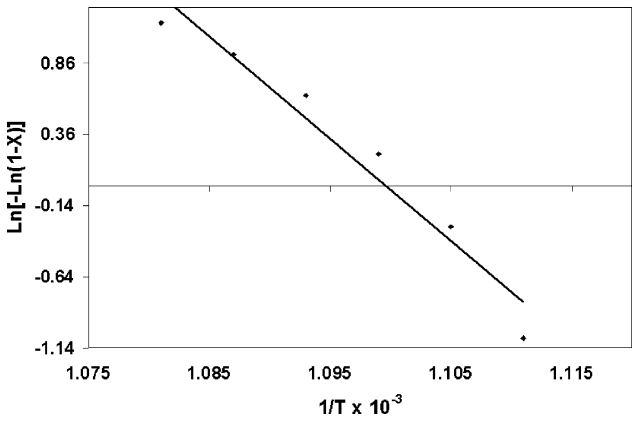

Fig. 4. Defermination of crystallization activation energy for AR-$Cr_3Fe_5Ti_5$ by Matusita method.

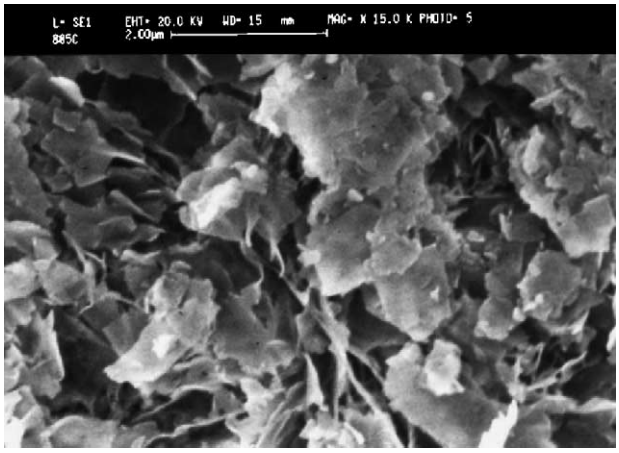

Fig. 5. SEM micrograph of AR-$Cr_3Fe_5Ti_5$ first nucleated at 740 °C for 3 h and then heated at 885 °C for 3 h.

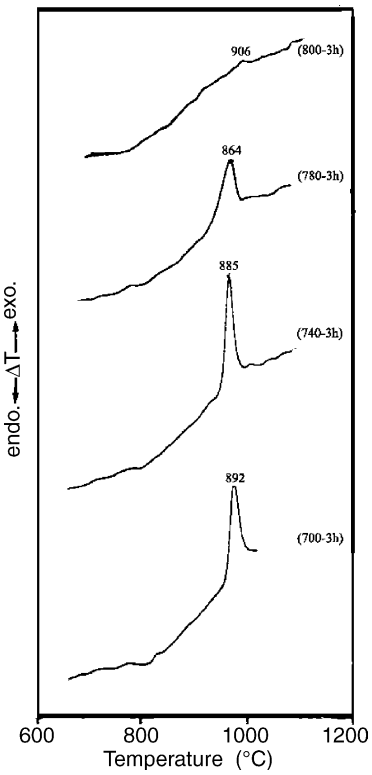

Fig. 6. DTA traces of AR-$Cr_3Fe_5Ti_5$ glass previously heat-treated at indicated temperatures for 3 h.

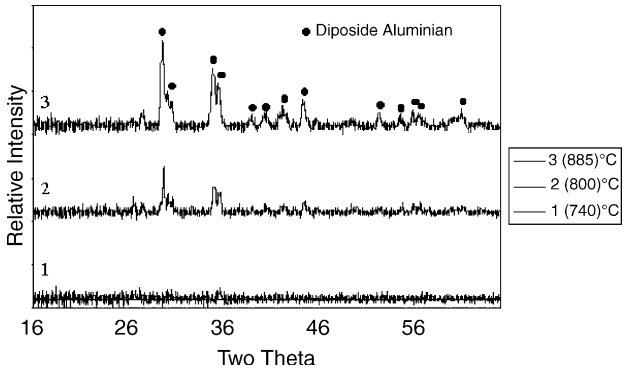

Fig. 7. XRD patterns of AR-$Cr_3Fe_5Ti_5$ heat-treated at 740, 800 and 885 °C for 3 h.

4. Conclusions

1. It seems that using a combination of Cr_2O_3, Fe_2O_3 and TiO_2 nucleating agents with weight parts of 3, 5 and 5, respectively, is most effective in inducing bulk crystallization in the specimens investigated herein.
2. For crystallization of the most promising specimens (AR-$Cr_3Fe_5Ti_5$) E and n values were determined as 253.60 and 3.23 kJ/mol, respectively. The Avrami constant indicating a two dimensional bulk crystallization mechanism, confirmed by SEM micrographs.
3. The most suitable nucleation temperature was determined as 740 °C for the most promising specimens. This specimen after a 3 h nucleation treatment at this temperature exhibited the sharpest and the lowest temperature exo-peak at 885 °C in subsequent DTA runs.

References

[1] L.I. Frantsenyuk, I.V. Blinstova, A.E. Seredkin, Synthesis of slag-glass ceramics, Glass Ceram. 53 (11/12) (1996) 356–361.
[2] L.J. Shelestak, R.A. Chavez, J.D. Mackenzie, Glasses and glass-ceramics from naturally occurring CaO–MgO–Al_2O_3–SiO_2 materials (I) glass formation and properties, J. Non-Cryst. Solids 27 (1978) 75–81.
[3] L.J. Shelestak, R.A. Chavez, J.D. Machenzie, Glasses and glass-ceramics from naturally occurring CaO–MgO–Al_2O_3–SiO_2 materials (II) crystallization behaviour, J. Non-Cryst. Solids 27 (1978) 83–97.
[4] G. Agarwal, K.S. Hong, M.R. Fletcher, R.F. Speyer, Crystallization behaviour of copola slag glass-ceramics, J. Non. Cryst. Solids 130 (1991) 187–197.
[5] G.H. Beall, H.L. Rittler, Basalt glass ceramics, Am. Ceram. Soc. Bull. 55 (6) (1978) 579–582.
[6] J.A. Topping, The fabrication of glass-ceramic materials based on blast furnace slag—a review, J. Can. Ceram. Soc. 45 (1976) 63–67.
[7] J. Williamson, The kinetics of crystal growth in an aluminosilicate glass containing small amounts of transition-metal ions, Min. Mag. 37 (291) (1970) 759–770.
[8] A. Omar, A.W. Elshennauri, G.A. Khater, The role of Cr_2O_3, LiF and their mixtures on crystalline phase formation and microstructure in Ba, Ca, Mg aluminosilicates glass, Br. Ceram. Trans. J. 90 (1991) 179–183.
[9] M.W. Davies, B. Kerrison, W.E. Gross, M.J. Robson, D.F. Wichall, Slag ceramics—a glass ceramic from blast-furnace slag, J. Iron Steel Inst. 208 (1970) 348–370.
[10] L. Barbieri, C. Leonelli, T. Manfredini, G.C. Pellacani, C. Siligardi, E. Tondello, R. Bertoncello, Solubility reactivity and nucleation effect of Cr_2O_3 in the CaO–MgO–Al_2O_3–SiO_2 glassy system, J. Mater. Sci. 29 (1994) 6273–6280.
[11] A. Karamanov, P. Pisciella, M. Pelino, The effect of Cr_2O_3 as a nucleating agent in iron-rich glass-ceramics, J. Eur. Ceram. Soc. 19 (1999) 2641–2645.
[12] V.K. Marghussian, S. Arjomandnia, Effect of Cr_2O_3 on nucleation of SiO_2–Al_2O_3–CaO–MgO (R_2O, Fe_2O_3, TiO_2) glass ceramics, Phys. Chem. Glass. 39 (4) (1998) 246–251.
[13] V.K. Marghussian, S. Arjomandnia, Crystallisation behaviour of SiO_2–Al_2O_3–CaO–MgO (R_2O, Fe_2O_3, TiO_2) glass ceramics in the presence of a Cr_2O_3 nucleant, Phys. Chem. Glass. 40 (6) (1999) 311–313.
[14] G. Baldi, E. Generali, Effects of nucleating agents on diopside crystallization in new glass-ceramics for tile-glaze application, J. Mater. Sci. 30 (1995) 3251–3255.
[15] R.G. Duan, K.M. Liang, S.R. Gu, Effect of changing TiO_2 content on structure and crystallization of CaO–Al_2O_3–SiO_2 system glasses, J. Eur. Ceram. Soc. 18 (1998) 1729–1735.
[16] S. Morimoto, N. Kuriyama, Effect of TiO_2, ZrO_2 and P_2O_5 on the crystallization of SiO_2–Al_2O_3–MgO–CaO–Na_2O glass system, J. Ceram. Soc. Jpn. 104 (5) (1996) 442–443.
[17] K. Matusita, T. Komatsu, R. Yokota, Kinetic of non-isothermal crystallization process and activation energy for crystal growth in amorphous materials, J. Mater. Sci. 19 (1984) 291–296.
[18] K. Matusita, S. Sakka, Kinetic study of the crystallization of glass by differential scanning calorimetry, Phys. Chem. Glass. 20 (4) (1979) 81–84.
[19] C.S. Ray, D.E. Day, Determining the nucleation rate curve for lithium disilicate glass by differential thermal analysis, J. Am. Ceram. Soc. 73 (2) (1990) 439–442.